# Effect of the micromoulding process conditions on polymer flow behavior within a variable thickness microcavity

T. V. Zhiltsova*; M.S.A. Oliveira; J.A. Ferreira

*Department of Mechanical Engineering, University of Aveiro, Portugal*

J.C.Vasco

*Polytechnic Institute of Leiria / Institute for Polymers and Composites/I3N University of Minho, Portugal*

A. S. Pouzada; A.J. Pontes

*Institute for Polymers and Composites/I3N University of Minho, Portugal*

ABSTRACT: Fast time to market along with high level of automation and versatility made microinjection moulding, by far, a favorite technique for the mass production of microplastic components. In the microimpressions, very high shear rates develop, eventually leading to excessive shear heating and consequently to less predictable flow behaviour comparing to conventional injection moulding. In this study, the flow behaviour within a variable thickness microimpression is investigated by monitoring pertinent process parameters such as cavity temperature and pressure. A micromoulding insert with a variable thickness was designed, fabricated and instrumented with pressure and temperature sensors. Full factorial design of experiment (DOE) was carried out to optimize the filling of the microimpression. The study with acrylonitrile butadiene styrene (ABS) suggests that the mould temperature plays an important role in the microimpression filling regardless of its thickness. In addition, the microinjection moulding process was monitored in terms of the cavity pressure and temperature, enabling closer assessment of the polymer flow state in the microimpression.

## 1 INTRODUCTION

In recent years microinjection moulding has been in continuous growth due to its ability to quickly and inexpensively produce large amounts of microparts. Besides the modification of the injection moulding equipment and moulds, downscaling of the macro-injection process also requires a thorough understanding of the physics underlying microinjection moulding. High surface-to-volume ratios in microparts require higher injection pressure and injection speed to prevent premature solidification. In these conditions, excessive shear and elongation stresses are likely to promote slippage of the polymer at the mould wall and deteriorating the quality of the micromouldings (Giboz et al. 2009; Vasco et al. 2010).

Recently it was attempted to find the influence of the injection moulding conditions on the surface quality of microparts. Preheating the mould above the glass transition temperature of polymer was reported to avoid short shots and improve the overall part quality (Liou and Chen 2006; Xie and Ziegmann 2009). Moreover, using the upper limit of the conventional mould temperature enhanced the replication of microfeatures for a wide range of polymers (Attia and Alcock 2009; Sha et al. 2007a). Considering the shear thinning behaviour of polymers, premature solidification could be reduced by some extent by injection at higher shear rates. Filling degree of micro pins was reported to be improved by injection at high injection velocity, having, on the other hand, an adverse effect on the surface finishing (Sha et al. 2007b). Combined effect of the high injection velocity and high melt temperature was found out to be significant, for good replication of the micro walls (Theilade and Hansen 2007).

Downscaling of the injection moulding process is an additional challenge to the microcomponent quality evaluation. In general this is rather qualitative than quantitative as micropart visual appearance and filling degree are often the main criteria used. However, if the evaluation is correlated solely to the injection moulding process conditions, it does not inform on the rheology of the polymer during filling; this can only be known by monitoring pertinent parameters such as cavity pressure and temperature. Monitoring of the micromoulding process is still a challenge, since the majority of sensors currently available are too big for the micromoulding size. To overcome these limitations, indirect monitoring has been used to gather information on temperature, heat flow, injection pressure, injection speed and displacement (Whiteside et al. 2004; Yan et al. 2003; Zhao et al. 2006).

The pressure sensor embedded into the plunger of the microinjection moulding machine was implemented to monitor the metering size and pressure evolution. However, it does not represent the poly-

mer behaviour inside the impression (Zhao et al. 2006). Cavity pressure monitoring is considered to be the better approach to verify the process variation. Yan and co-workers implemented a single-axis force sensor, embedded into the knock out mechanism, for monitoring cavity pressure (Yan et al. 2003). In another research, a piezoelectric force transducer is positioned behind the cavity ejector pin to indicate the progress of filling and the part solidification time (Whiteside et al. 2004). With respect to the mould temperature J-type thermocouples, embedded at few millimetres in the cavity wall, made it possible to indirectly monitor the polymer temperature and solidification (Whiteside et al. 2003; Whiteside et al. 2004).

Although some reliable data about the temperature and pressure evolution has been reported, so far the majority of current sensors can hardly meet requirements as contact area below 1 $mm^2$ (Luo and Pan 2007; Ono et al. 2007). With further sensor miniaturization it will be possible to collect pressure and temperature data, namely, in microimpressions with variable thickness.

In this study, polymer flow dynamics within a variable thickness microimpression is investigated by monitoring temperature and pressure. An optimization of the microimpression filling was performed by Taguchi design of experiment (DOE) with a subsequent analysis of the deviation of the peak cavity temperature from the desired values. In addition, the sensors located at definite distances in the flow path allow monitoring the flow front progress and how the melt speed may be affected.

## 2 EXPERIMENTAL SET UP

### 2.1 *Experimental equipment*

The mouldings were produced with a Boy 12 A injection moulding machine with Ø14 mm screw (Dr Boy, Germany). This machine can meter an injection volume of 100 $mm^3$ at flow rate up to 15.6 $cm^3.s^{-1}$. The injection pressure is limited to 240 MPa. A mould temperature regulator and an external control unit for the cartridge heaters were used for controlling the mould temperature.

### 2.2 *Micromoulding details*

The micromould used in this work accommodates an interchangeable moulding block (Vasco et al. 2009). The one used in this study features a 16 mm by 10 mm plate-like cavity with a central aperture. The cavity was manufactured by micro-milling. The thicknesses in the impression are of 200, 300 and 400 µm. The layout of the moulding is shown in Fig. 1.

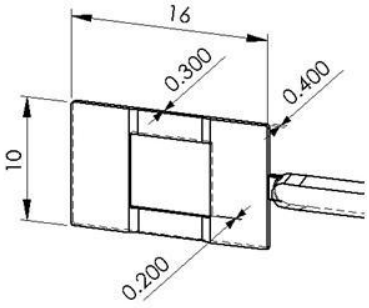


Figure1. Micropart details (dimensions in mm).

### 2.3 *Data acquisition*

The melt flow was monitored with temperature and pressure sensors. The pressure sensors are miniature piezoelectric Priamus 6006B (Priamus System Technologies, Switzerland). The first pressure sensor is mounted near the gate and the second at the end of the flow path. Two temperature microsensors Priamus 4011B with contact diameter of 600 µm were flash-mounted at the zones of the microimpression with thicknesses of 300 and 200 µm. The location of the sensors is depicted in Fig. 2; hereforth they are designated as: P1-pressure sensor near the gate; P2- pressure sensor at the end of flow path; T1-temperature sensor at the 300 µm thick zone; T2-temperature sensor at the 200 µm zone.

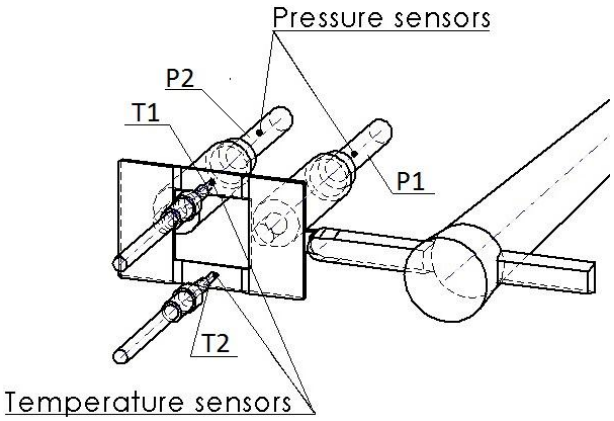


Figure 2. Layout of the micropart with pressure and temperature sensors

The data acquisition system consisted of the input module Multi DAQ 8101 A, which cyclically records pressure and temperature data at sample rates of 1 kHz, and the amplifier module Mobile DAQ 8001B, both from Priamus. The user interface was based on the Priamus Moulding Monitor software.

### 2.4 *Materials*

An amorphous polymer acrylonitrile butadiene styrene (ABS) Cycolac GPM 5500S, by SABIC, was used. It has a wide processing window with MFR of 24 g/10 min (220°C, 10 kg). Prior to processing, the material was dried during two hours at 85°C.

## 2.5 *Experimental procedure*

Full factorial design of experiment (DOE) was carried out to optimize the filling of the variable thickness microcavity. The parameters selected to be studied within DOE were the barrel temperature ($T_b$), the mould temperature (Tm) and the injection speed ($V_j$), varied at two levels: 1- low and 2- high, giving $2^3$ runs. The combination of controlled parameters is presented in Table 1.

Table 1. Combination of the controlled parameters for L8 orthogonal array

| *Experiment Nº* | *Mould temperature (℃)* | *Melt temperature (℃)* | *Injection velocity (mm/s)* |
|---|---|---|---|
| 1 | 75 | 210 | 72 |
| 2 | | | 144 |
| 3 | | 250 | 72 |
| 4 | | | 144 |
| 5 | 95 | 210 | 72 |
| 6 | | | 144 |
| 7 | | 250 | 72 |
| 8 | | | 144 |

The other processing parameters were the same for all experiments: injection pressure 150 MPa, holding pressure 45 MPa and holding time 2 s. In each experiment 10 mouldings were discarded before collecting 35 microparts and recording the pressure and temperature data.

## 2.6 *Pressure and temperature data*

Injection moulding is a process prone to some variability caused by ambient temperature, air humidity, delayed response of injection moulding machine and variations of the cylinder temperature (Osswald et al. 2008). At the microscale, the effects of these factors and/or their combinations are amplified due to the tiny dosage of polymer melt. This may affect the polymer viscosity in a way that occasionally leads to unacceptable defective mouldings.

During the experimental runs, some injection cycles resulted in short shots. In order to exclude the these incomplete mouldings, all pressure and temperature data were processed with MATLAB. A filtering algorithm was assigned to automatically remove all the cycles when the peak pressure didn't reach 100 bar. This criterion guaranties that only pressure and temperature data for complete micromouldings will be considered in future analyses. The ratio of the recorded cycles to the post-processed ones shows the natural variability of the microinjection moulding process and is given by:

$$\frac{N_{c.f.}}{N_{c.r.}} \times 100 \qquad (1)$$

where $N_{c.f}$ is the number of filtered cycles, and $N_{c.r}$ is the number of recorded cycles.

The results of calculations for 8 injection moulding setups are summarized in Table 2, where the higher percentage means less process variability.

Table 2. Ratio of the filtered to recorded injection moulding cycles

| DOE | Number of cycles | | Ratio of acceptance (%) |
|---|---|---|---|
| | $N_{c.r}$ | $N_{c.f}$ | |
| 1 | 35 | 31 | 89 |
| 2 | | 33 | 94 |
| 3 | | 26 | 74 |
| 4 | | 29 | 83 |
| 5 | | 31 | 89 |
| 6 | | 29 | 83 |
| 7 | | 28 | 80 |
| 8 | | 32 | 91 |

After processing the pressure and temperature data, 25 cycles for each injection run were randomly selected for evaluation of the injection moulding processing conditions effect on the flow front advancement.

# 3 RESULTS AND DISCUSSIONS

## 3.1 *Evaluation of the polymer melt dynamics*

The configuration of the pressure and temperature sensors, depicted on Fig. 2, allows the monitoring of the flow front progress. As soon as polymer melt arrives at the sensor locations the temperature or pressure profiles start to build up. From the time intervals required for the melt to reach from one sensor to another, it is possible to assess how the microimpression is filled. Typical temperature and pressure profiles are shown in Figure 3.

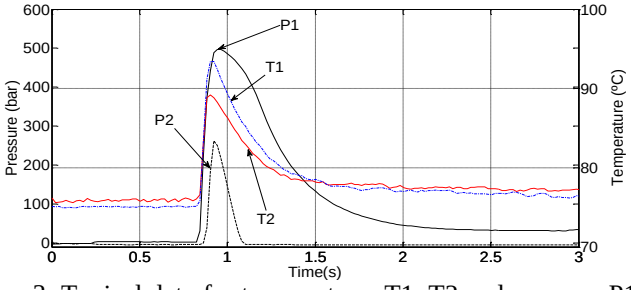


Figure3. Typical data for temperature: T1, T2 and pressure P1, P2 (injection moulding processing conditions DOE 7).

During filling of the microimpression, three time intervals were defined: P1-T1, P1-T2 and T1-P2. The former intervals represent times required for polymer flow to travel from the pressure sensor P1 to the temperature sensors T1 (300 µm section) and T2 (200 µm section) respectively, while the latter describes the time for the melt flow from T1 to P2. The reason for assuming that P2 is touched by the flow front arriving from the 300 µm section may be explained by the differential thickness of the micromoulding and respective asymmetry of the weld line position. In Fig. 4, showing a short shot, it can

be clearly seen that polymer flow reached P2 at the thicker (300 μm) section of the impression.

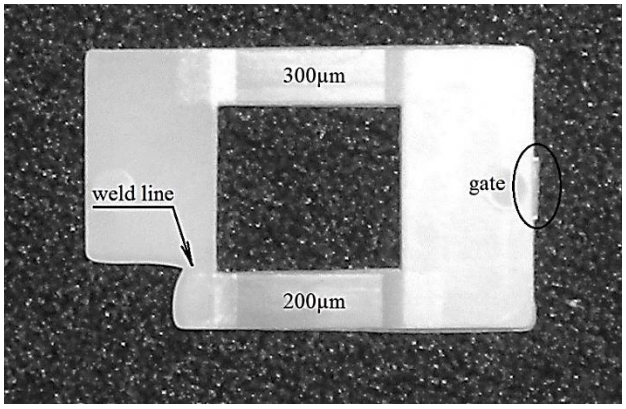


Figure 4. Short shot of the micropart (injection moulding processing conditions DOE 7)

A comparison of the P1-T1 and P1-T2 time intervals is shown in Fig. 5. In all moulding runs the flow takes longer to reach T2 at the 200 μm section, due to the slower speed at the thinner section. When the thickness is reduced, the cooling rate increases as well as the viscosity. As expected, both P1-T1 and P1-T2 time intervals reflect the change of the injection speed, according to the conditions in Table 1. Moreover, when the injection velocity increases, the difference between the P1-T1 and P1-T2 time intervals to some was degree reduced (DOE2, DOE4, DOE 6 and DOE8), indicating a viscosity reduction.

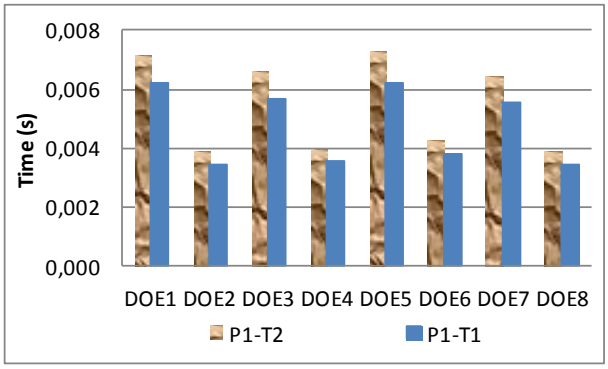


Figure 5. Time intervals for flow front advancement between P1-T1 and P1-T2.

This decreasing tendency was also verified when the melt temperature increased at low injection velocity (DOE 3 and 7). Nevertheless, in the DOE 6 injection run, the time intervals are out of the typical variation pattern, slightly longer than with identical injection speed conditions. This may be ultimately attributed to some natural process variations responsible for an increase of melt viscosity.

A comparison of the time intervals P1-T1 and T1-P2 is shown in Fig. 6. As depicted in Fig. 2, the sensor T1 is equidistantly located from the sensors P1 and P2, through the length of the microimpression. As it should be expected, the time intervals T1-P2 for all injection runs are longer than the P1-T1.

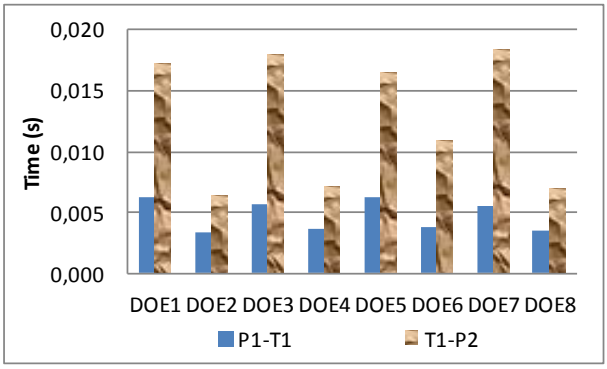


Figure 6. Time intervals for flow front advancement between P1-T1 and T1-P2.

These time differences suggest that the melt cools quickly and the flow front advancement becomes slower as it progresses inside the microimpression (i.e. which corresponds to an increase in the time required for the melt flow reach from T1 to P2). These differences seem quite significant, since they are approximately twice longer for higher injection velocity (DOE 2, 4, 6 and 8) and three times longer for lower injection velocity (DOE 1, 3, 5 and 7). It would be interesting to compare our data with those obtained by numerical simulation to understand how the magnitude of the heat transfer coefficient at the plastic-mould interface may affect the filling of the microimpression. In the commercial simulation codes, the latter is generally assumed to be constant during the injection stage, regardless of the cavity thickness. However, Nguyen-Chung reports the heat transfer coefficient to vary with respect to injection speed and thickness (Nguyen-Chung et al. 2010). For the sake of accuracy improvement of the simulation, this aspect deserves further investigation. Apparently, neither the mould nor the melt temperatures seem to have a definite effect on the melt flow velocity from the middle sections to the end of the flow path. In addition, for the processing conditions DOE6, the interval T1-P2 does not fall into the pattern previously observed for the other injection runs with higher injection velocity. The latter, was found out to be somehow longer and therefore indicating a lower velocity. In order to comprehend the reason for this delay, the latter has to be compared with the peak cavity temperature at the same test conditions.

### 3.2 *Assessment of the cavity temperature*

The recorded temperature is actually lower than the real melt temperature within the cavity due to the high cooling rate in the microimpression and hence, the delayed response of the temperature sensors. Nevertheless, it shows an evolution of the melt temperature at the mould/melt interface. Typical temperature profiles for the 200 μm and 300 μm sections at DOE 7 processing conditions ($T_{inj}$=210ºC; $T_{mould}$= 95ºC; $v_{inj}$= 72 mm/s) are shown in Fig. 7.

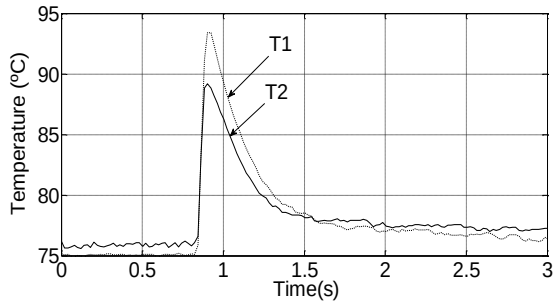


Figure7. Typical cavity temperature profiles: T1-300µm, T2-200µm (injection moulding processing conditions DOE 7)

The peak temperature values from DOE1 through DOE8 are shown in Fig. 8. To minimize the measurement error, the average over 25 injection moulding cycles was used for comparison purposes. For all eight sets of the processing conditions, the peak temperature at the thicker section is higher than at the thinner one, resulting from faster cooling of the melt caused by the smaller thickness. Shear heating of the melt also contributes for a slight increase of the peak cavity temperature with an increase of the injection velocity (DOE 2, 4, 8). This effect seems to be more prominent in DOE 2, where the melt and mould temperatures were at the lowest levels. However, for higher mould temperature, low melt temperature and high injection speed (DOE 6), both peak cavity temperatures were slightly lower than for DOE 5 with the same melt and mould temperature but slower injection velocity. This observation is consistent with the time interval data on Fig. 5 and 6. It should also be said that the latter was found out to be longer than expected for the high injection velocity condition and may be an indication of external interferences on the process.

Any experimental results are highly affected by numerous internal and external disturbances, so-called noise factors. The influence of this noise on the outcome of the experiments, is measured by the signal to noise (S/N) ratio (Roy 2010). Higher values of the S/N ratio mean that the influence of input signal is higher than disturbances of the experiments. In this work, the desired value is the maximum peak cavity temperature. As it has been mentioned earlier, at higher cavity temperature the microimpression is more easily filled due to the reduction of the melt viscosity. Therefore, a S/N ratio for larger-the-better quality criterion was adopted. The SN ratio (larger-the-better) in the *i*th experiment can be expressed as:

$$SN = -10 \times log\left(\frac{1}{n} \times \sum_{i=1}^{n} \frac{1}{y^2}\right) \qquad (2)$$

where *i* is the experiment number, *y* is the data and *n* is the number of the trials in each experiment.

The results of the calculations of the average S/N levels are summarized in Fig. 9 and 10. The highest value of the S/N response for each factor indicates the best combination of parameters for the maximum cavity temperature. Furthermore, the difference between the maximum and minimum levels shows the influence of each factor on the peak cavity temperature at the 200 and 300 µm thick cavity sections.

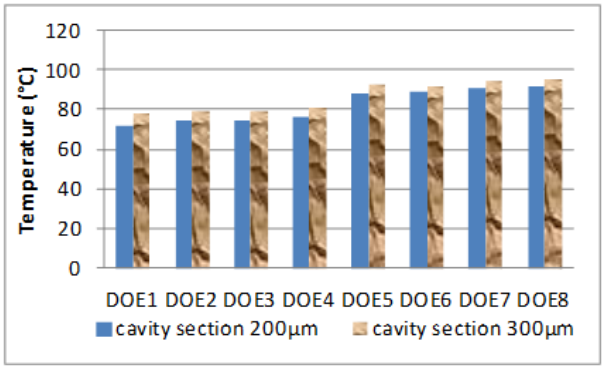


Figure 8. Peak cavity temperatures at the micropart sections of 200µm and 300µm

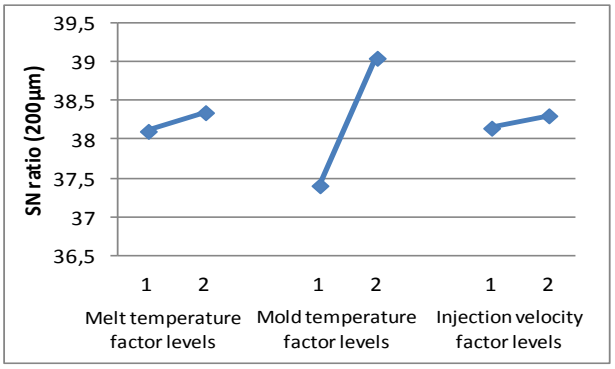


Fig.9 SN response for the cavity temperature at the 200 µm thick section

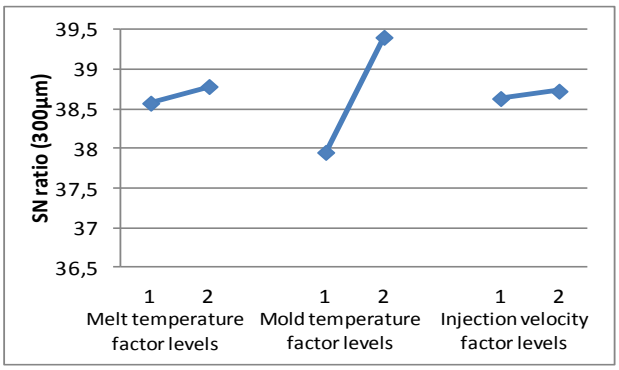


Fig.10 SN response for the cavity temperature at the 200 µm thick section.

As depicted in Fig. 11, the two levels difference highlights the mould temperature as the most influencing factor for the maximum cavity temperature for both 200 and 300 µm thick sections, while the melt temperature appears to have a similar but lower effect. To a large degree, both mould and melt temperatures appear to determine the peak temperature at the thinner section. The injection speed seems to increase the peak cavity temperature at lesser degree, being at the lowest levels. However, it has almost a doubled influence at the 200 µm section.

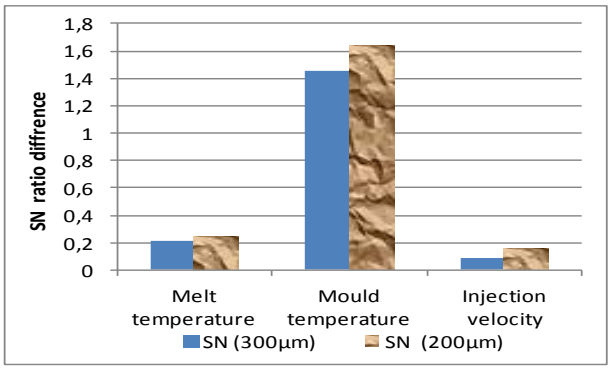

Fig.11 SN difference for the peak cavity temperature at 300µm and 200 µm sections

## 4 CONCLUSIONS

Full factorial design of experiment (DOE) has been carried out to explore the effect of injection moulding processing conditions and micromoulding thickness on the melt dynamics. Experimental data were gathered in an instrumented mould with pressure and temperature sensors.

For all processing conditions, the polymer flows slowly at the thinner 200 µm section due to the higher cooling rates and the increase in viscosity. It was also confirmed that the melt cools significantly farther from the gate, the cooling rate varying not only with thickness but also with the injection speed.

The higher mould temperature is detrimental for optimizing the peak cavity temperature. Moreover, this effect was more accentuated at the thinner section. The peak cavity temperature also increases when the melt temperature and injection velocity are higher, but these factors were less influent on the peak cavity temperature than the mould temperature.

The variability of the microinjection moulding process was evaluated in terms of completeness of the micromouldings. The accepted micropart rate varies between 74% and 94%, but it was not possible to discern any definite tendency, in spite of the maximum incidence occurring at slower injection speed.

## ACKNOWLEDMENTS

The authors acknowledge the support of Fundação para a Ciência e Tecnologia, Portugal, through the project PTDC/EME/TME/66227/2006 and the PhD Individual Grant SFRH/BP/45585/2008.

## REFERENCES

Attia, U. & Alcock, J. 2009. An evaluation of process-parameter and part-geometry effects on the quality of filling in micro-injection moulding. *Microsystem Technologies* **15** (12): 1861-1872.

Giboz, J., Copponnex, T. & Mélé, P. 2009. Microinjection molding of thermoplastic polymers: morphological comparison with conventional injection molding *Journal of Micromechanics and Microengineering* **19** (2).

Liou, A. C. & Chen, R. H. 2006. Injection molding of polymer micro- and sub-micron structures with high-aspect ratios. *The International Journal of Advanced Manufacturing Technology* **28** (11): 1097-1103.

Luo, R. C. & Pan, Y. L. 2007. Rapid Manufacturing of Intelligent Mold with Embedded Microsensors. *IEEE/ASME Transactions on Mechatronics* **12** (2): 190-197.

Nguyen-Chung, T., Jüttner, G., Löser, C., Pham, T. & Gehde, M. 2010. Determination of the heat transfer coefficient from short-shots studies and precise simulation of microinjection molding. *Polymer Engineering & Science* **50** (1): 165-173.

Ono, Y., Whiteside, B. R., Brown, E. C., Kobayashi, M., Cheng, C.-C., Jen, C.-K. & Coates, P. D. 2007. Real-time process monitoring of micromoulding using integrated ultrasonic sensors. *Transactions of the Institute of Measurement and Control* **29** (5): 383-401.

Osswald, T. A., Turng, L. S. & Gramann, P. J. 2008. *Injection Moulding Handbook*, Muench: Hanser

Roy, R. K. 2010. "A Primer on the Taguchi Method." SME, Dearborn, Michigan, 297.

Sha, B., Dimov, S., Griffiths, C. & Packianather, M. 2007a. Micro-injection moulding: Factors affecting the achievable aspect ratios. *The International Journal of Advanced Manufacturing Technology* **33** (1): 147-156.

Sha, B., Dimov, S., Griffiths, C. & Packianather, M. S. 2007b. Investigation of micro-injection moulding: Factors affecting the replication quality. *Journal of Materials Processing Technology* **183** (2–3): 284-296.

Theilade, U. & Hansen, H. 2007. Surface microstructure replication in injection molding. *The International Journal of Advanced Manufacturing Technology* **33** (1): 157-166.

Vasco, J., Maia, J. M. & Pouzada, A. S. 2010. Microinjection moulding–Wall-slip evaluation of POM flow in microchannels. In *PPS 26th Ann. Meeting*; Banff, Canada, July, 2010.

Vasco, J. C., Maia, J. M. & Pouzada, A. S. 2009. Thermo-rheological behaviour of polymer melts in microinjection moulding. *Journal of Micromechanics and Microengineering* **19** (10).

Whiteside, B. R., Martyn, M. T., Coates, P. D., Allan, P. S., Hornsby, P. R. & Greenway, G. 2003. Micromoulding: process characteristics and product properties. *Plastics, Rubber and Composites* **32** (6): 231-239.

Whiteside, B. R., Martyn, M. T., Coates, P. D., Greenway, G., Allen, P. & Hornsby, P. 2004. Micromoulding: process measurements, product morphology and properties. *Plastics, Rubber and Composites* **33** (1): 11-17.

Xie, L. & Ziegmann, G. 2009. Influence of processing parameters on micro injection molded weld line mechanical properties of polypropylene (PP). *Microsystem Technologies* **15** (9): 1427-1435.

Yan, C., Nakao, M., Go, T., Matsumoto, K. & Hatamura, Y. 2003. Injection molding for microstructures

controlling mold-core extrusion and cavity heat-flux. *Microsystem Technologies* **9** (3): 188-191.

Zhao, J., Lu, X. H., Chen, G., Liu, S. L., Juay, Y. K. & Yong, M. S. 2006. Micromold filling behavior studies of polymer materials. *Materials Research Innovations* **10** (4): 394-397.